

# Lawrence Berkeley National Laboratory

## LBL Publications

### Title

Some Aspects of the Two Beam Performance of DCI

### Permalink

<https://escholarship.org/uc/item/02z7d2jv>

### Authors

Krishnagopal, S

Siemann, R

### Publication Date

1991-09-01



# Lawrence Berkeley Laboratory

UNIVERSITY OF CALIFORNIA

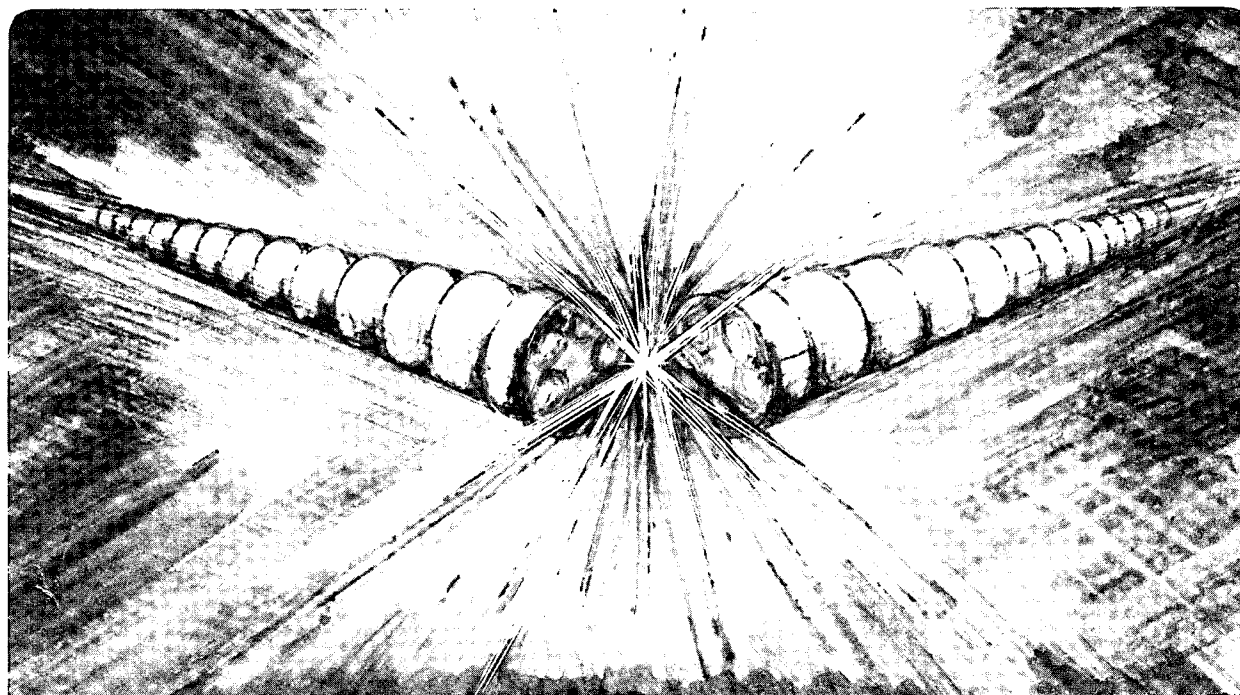
## Accelerator & Fusion Research Division

Submitted to Nuclear Instruments and Methods A

### Some Aspects of the Two Beam Performance of DCI

S. Krishnagopal and R. Siemann

September 1991



LOAN COPY |  
Circulates |  
for 4 weeks | Bldg. 50 Library.  
Copy 2

LBL-31227

#### DISCLAIMER

This document was prepared as an account of work sponsored by the United States Government. Neither the United States Government nor any agency thereof, nor The Regents of the University of California, nor any of their employees, makes any warranty, express or implied, or assumes any legal liability or responsibility for the accuracy, completeness, or usefulness of any information, apparatus, product, or process disclosed, or represents that its use would not infringe privately owned rights. Reference herein to any specific commercial product, process, or service by its trade name, trademark, manufacturer, or otherwise, does not necessarily constitute or imply its endorsement, recommendation, or favoring by the United States Government or any agency thereof, or The Regents of the University of California. The views and opinions of authors expressed herein do not necessarily state or reflect those of the United States Government or any agency thereof or The Regents of the University of California and shall not be used for advertising or product endorsement purposes.

Lawrence Berkeley Laboratory is an equal opportunity employer.

## **DISCLAIMER**

This document was prepared as an account of work sponsored by the United States Government. While this document is believed to contain correct information, neither the United States Government nor any agency thereof, nor the Regents of the University of California, nor any of their employees, makes any warranty, express or implied, or assumes any legal responsibility for the accuracy, completeness, or usefulness of any information, apparatus, product, or process disclosed, or represents that its use would not infringe privately owned rights. Reference herein to any specific commercial product, process, or service by its trade name, trademark, manufacturer, or otherwise, does not necessarily constitute or imply its endorsement, recommendation, or favoring by the United States Government or any agency thereof, or the Regents of the University of California. The views and opinions of authors expressed herein do not necessarily state or reflect those of the United States Government or any agency thereof or the Regents of the University of California.

LBL-31227  
ESG Note-154  
SLAC-PUB-5653

**Some Aspects of the Two Beam Performance of DCI\***

**S. Krishnagopal**

**Lawrence Berkeley Laboratory  
University of California  
Berkeley, CA 94720**

**and**

**R. Siemann**

**Stanford Linear Accelerator Center  
Stanford University  
Stanford, CA 94309**

**Submitted to Nuclear Institute and Methods**

**\*This work was supported by the Director, Office of Energy Research, Office of High Energy and Nuclear Physics, High Energy Physics Division, of the U.S. Department of Energy under Contract No. DE-AC03-76SF00098.**

## Some Aspects of the Two Beam Performance of DCI

S. Krishnagopal

*Lawrence Berkeley Laboratory, University of California, Berkeley, CA 94720*

R. Siemann

*Stanford Linear Accelerator Center, Stanford University, Stanford, CA 94309*

**ABSTRACT:** The results of beam-beam simulations that model DCI operating as an  $e^+e^-$  collider are reported. The simulation techniques, including a new procedure for incorporating synchrotron radiation, are described. Phase advance errors between the interaction points explain the beam-beam limit at the operating point  $q_x = q_y = 0.725$  ( $q$  denotes the fractional part of the tune). The effects of radiation damping are also studied near that operating point. Simulation and experiments disagree in a second operating region,  $q_x = q_y \sim 0.795$ , indicating additional physics outside the scope of our model.

### I. INTRODUCTION

We have conjectured that the beam-beam performance of  $e^+e^-$  storage ring colliders could be enhanced by operating with a round rather than the more conventional flat collision spot[1]. This conjecture was motivated in part by the work of Peggs and Talman on beam-beam driven resonances[2] and is supported by computer simulations in Ref. 1. The DCI storage ring[3] that operated at Laboratoire de l'Accélérateur Linéaire (Orsay, France) about 10 years ago was close to a round beam collider. DCI did not achieve the beam-beam performance that we would have hoped. This could be attributed to a number of factors ranging from particular features of DCI to our conjecture being wrong. The latter makes understanding the performance of DCI part of our continuing work.

In this paper we use simulations to study the effects of synchrotron radiation damping and phase advance errors between interaction regions. We obtain agreement with DCI measurements at one operating point ( $q_x = q_y = 0.725$ ) but not in a second operating region ( $q_x = q_y \sim 0.795$ ). We assume *implicitly* that the beam-beam limit is a single-particle, incoherent phenomenon in this and earlier work, but this may not be the case[4]. We present some preliminary evidence that the disagreement at  $q_x = q_y \sim 0.795$  could be due to coherent beam-beam effects.

The luminosity of a collider is

$$\mathcal{L} = \frac{1}{4\pi} \frac{N^2 f_c}{\sigma_x \sigma_y} \quad (1)$$

where  $N$  is the number of particles per bunch (assumed equal for the two beams),  $f_c$  is the collision frequency, and  $\sigma_x$  and  $\sigma_y$  are the rms horizontal and vertical sizes at the collision point. The beam is flat in most  $e^+e^-$  storage rings,  $R_\sigma = \sigma_y/\sigma_x \ll 1$ [5]. The strength of the beam-beam interaction is measured by the beam-beam strength parameters

$$\xi_j = \frac{r_e}{2\pi} \frac{N \beta_j^*}{\gamma \sigma_j (\sigma_x + \sigma_y)} \quad j = x, y \quad (2)$$

In this equation  $\beta_x^*$  and  $\beta_y^*$  are the betatron amplitude functions at the interaction region (IR),  $\gamma$  is the energy in units of  $mc^2$ , and  $r_e$  is the classical electron radius. If there is no dispersion at the IR and  $\beta_y^* = R_\sigma \beta_x^*$ , then  $\xi_x = \xi_y = \xi$  and the luminosity can be written

$$\mathcal{L} = \frac{I \gamma \xi}{2e r_e \beta_y^*} (1 + R_\sigma) \quad (3)$$

where  $e$  is the electron charge and  $I$  is the total current.

The  $(1 + R_\sigma)$  in eq. (3) is one factor that favors round beams, but our conjecture is that there is an *additional* factor related to  $\xi$ [1]. Specifically, the maximum beam-beam strength reached in simulations is  $\xi > 0.10$  when: i)  $R_\sigma = 1$ , ii)  $\beta_x^* = \beta_y^*$ , iii) the horizontal and vertical tunes,  $Q_x$  and  $Q_y$ , are equal, iv) the tunes have fractional parts just above 1/4, 1/2, or 3/4, v) the vertical emittance is made by random processes rather than coupling, vi) the fractional energy

loss between collisions is about  $10^{-4}$  (typical for a heavy quark factory), and vii) synchrotron motion is neglected[1]. As discussed in Section II points i), ii), iii) and vii) hold to a substantive degree for DCI, but iv), v) and vi) do not. In addition, DCI had two IR's; this introduces the possibility of optical errors that were not included in Ref. 1 because a one IR configuration typical of a heavy quark factory was studied there.

## II. DCI AND SIMULATION MODELS

DCI was an ambitious project aimed principally at testing ideas of beam-beam compensation by colliding four beams[6,7]. This design goal led to its having many of the features of a round beam collider including operating points near the coupling resonance,  $q_y = q_x$  ( $q$  denotes the fractional part of the tune), equal horizontal and vertical  $\beta^*$ 's, and, with full coupling,  $R_\sigma \sim 0.94$ [5]. These are the reason for our interest in the two beam,  $e^+e^-$ , performance. This paper considers the two beam performance exclusively[6,7].

Some features of DCI were not those of an ideal round beam collider. First, there are contributions to the beam sizes from dispersion. When the beam is fully coupled, the ratios of energy to betatron sizes are 0.40 in the vertical and 0.12 in the horizontal. Second, the emittance comes from coupling rather than random processes. This is discussed in Section IV.2; it was found to be unimportant. In addition, there are variables that could be important when extrapolating DCI performance to projected machines. These include the fractional energy loss between collisions (the damping decrement) and the number of interaction regions. They are investigated in detail in Section IV.

DCI parameters are given in Table I. The table also has the parameters of two models of DCI, ONE and TWO, that are used in the simulations reported in this paper. The differences between ONE and TWO in the order of importance are: i) the number of interaction regions (given by the names), ii) the energies, and iii) the circumferences. Optical errors were studied with TWO, and work on radiation damping was done with ONE. The ratio of nominal emittances is  $\epsilon_{TWO}/\epsilon_{ONE} = 0.64$ , and to reach the same  $\xi$ 's, the currents should be in the ratio  $I_{TWO}/I_{ONE} = 0.256$ .



There are two much more important differences between DCI and either model. The first is that synchrotron oscillations are neglected in the models. Synchrotron motion could influence the beam-beam performance through dispersion at the IR or tune modulation[8]. DCI had horizontal and vertical dispersion at the IR's, but, as discussed earlier in this section, the spot size was dominated by betatron motion. The ratio of bunch length to  $\beta^*$  at 1 GeV was 0.045, so tune modulation effects are negligible[9]. These arguments, plus the fact that the DCI group does not recall the synchrotron tune influencing the beam-beam performance[10], have led us to neglect synchrotron motion in the models.

The other major difference is that the models used a smooth approximation, described below, for the lattice focusing and coupling. With this approximation it is possible to simulate the effects of coupling on emittance, but we are taking a specific model for the coupling. This isn't an unreasonable approximation because the cause of residual coupling usually isn't known, but it is an approximation with some uncertain consequences. One consequence that should not be important is that the integer parts of  $Q_x$  and  $Q_y$  must be equal in the models.

### III. SIMULATION TECHNIQUE

One thousand test particles were tracked in models that had the beam-beam interaction and linear arcs as the main elements. Non-linear kicks were applied in the beam-beam interaction. Particle transport between collisions and synchrotron radiation took place in the arcs. The simulation was strong-strong; i.e. there were two beams and the beam sizes and centroid positions evolved turn-by-turn. A turn began with the particles half-way through the beam-beam interaction because this symmetry point is a natural location for calculating beam properties. (The beam-beam kicks from the first half of the interaction were stored and applied again after beam properties were calculated.)

#### III.1 *Beam-Beam Interaction*

The test particle coordinates are  $x_{bm}$  and  $y_{bm}$  where  $x$  and  $y$  are the horizontal and vertical, respectively. The first index  $b = 1, 2$  denotes the beam, and the second index  $m =$

1,...,M (M = 1000) denotes the test particle number. The mean positions and rms sizes were calculated from the test particle coordinates just before the beam-beam kick was applied. For example

$$\langle x_1 \rangle = \frac{1}{M} \sum_{m=1}^M x_{1m} ; \sigma_{x1} = \left[ \frac{1}{M} \sum_{m=1}^M (x_{1m} - \langle x_1 \rangle)^2 \right]^{1/2} . \quad (4)$$

These were used in calculating the beam-beam kicks. "Feedback" that set  $\langle x_1 \rangle = 0$ ,  $\langle x_2 \rangle = 0$ ,  $\langle y_1 \rangle = 0$ , and  $\langle y_2 \rangle = 0$  was used in some cases to adjust the mean positions before collisions.

The beams were treated as Gaussian in x and y, and the kicks were calculated for one-half of the interaction and applied twice. Assuming for the moment that  $\sigma_{x1} > \sigma_{y1}$ , the kicks for a particle in beam 2 were given by[11]

$$\Delta x_{2m} = \frac{-N r e^{\sqrt{\pi}}}{y \sigma_{d1}} \text{Im} \{ f_2(x_{2m} - \langle x_1 \rangle, y_{2m} - \langle y_1 \rangle) \} \quad (5a)$$

$$\Delta y_{2m} = \frac{-N r e^{\sqrt{\pi}}}{y \sigma_{d1}} \text{Re} \{ f_2(x_{2m} - \langle x_1 \rangle, y_{2m} - \langle y_1 \rangle) \}$$

where

$$f_2(x, y) = W \left[ \frac{x + iy}{\sigma_{d1}} \right] - \exp \left[ - \left\{ \frac{x^2}{2\sigma_{x1}^2} + \frac{y^2}{2\sigma_{y1}^2} \right\} \right] W \left[ \frac{xR_{\sigma1} + iy/R_{\sigma1}}{\sigma_{d1}} \right] \quad (5b)$$

In eqs. (5) N is the number of particles the beam,  $\sigma_{d1}^2 = 2(\sigma_{x1}^2 - \sigma_{y1}^2)$ ,  $R_{\sigma1} = \sigma_{y1}/\sigma_{x1}$ , and W is the complex error function.

Nominally the beams were round so  $\sigma_{y1} > \sigma_{x1}$  was as likely as  $\sigma_{x1} > \sigma_{y1}$ . If the former was the case, eqs. (5) were used with x and y interchanged everywhere. The program[12] that calculated  $W(z_R + iz_I)$  used an asymptotic expansion[13] when  $|z_R|$  and  $|z_I|$  were large (as they are when  $\sigma_{x1} \sim \sigma_{y1}$ ); this expansion is a good approximation and does not have numerical problems. In the case where  $\sigma_{x1} = \sigma_{y1}$  an asymptotic expansion of the complementary error function,  $\text{erfc}(z)$ , was used[14]; it gave

$$f_2(x, y) = \frac{i}{x+iy} \left[ 1 - \exp\left(-\frac{(x^2+y^2)}{2\sigma_{x1}^2}\right) \right] . \quad (6)$$

The text above describes the calculation of the beam-beam interaction for particles in beam 2. The same method was used for particles in beam 1.

These expressions assume that the beam distribution can be approximated as Gaussian for the purpose of calculating the electromagnetic fields produced. We have shown in a recent paper that this assumption prevents the appearance of some coherent beam-beam resonances[4]. Therefore, the restriction amounts to an *implicit* assumption that the dominant beam-beam effect is due to single particle, incoherent phenomena.

### III.2 Radiation

The arcs were treated as a linear transport with radiation damping and fluctuations. The simulation technique was motivated by work of Schonfeld[15] and is described in detail in earlier notes[16]. The phase space coordinates of a particle immediately after the beam-beam interaction and before entering the arc are represented as a vector  $\mathbf{x}_0 = (x_0, x'_0, y_0, y'_0)^T \equiv (x_{0i})^T$ . If an ensemble of particles were started at  $\mathbf{x}_0$ , the average phase space vector at the end of the arc would be  $\langle \mathbf{x} \rangle = (\langle x \rangle, \langle x' \rangle, \langle y \rangle, \langle y' \rangle)^T \equiv (\langle x_i \rangle)^T$ , and there would be deviations from  $\langle \mathbf{x} \rangle$  due to fluctuations. These deviations are given by a matrix  $S$  where

$$S_{ij} = \langle x_i x_j \rangle - \langle x_i \rangle \langle x_j \rangle \quad i, j = 1, \dots, 4 . \quad (7)$$

The properties and parameters of the arc determine  $\langle \mathbf{x} \rangle$  and  $S$ , and given these  $\mathbf{x}$ , the final phase space vector, can be calculated. It is centered at  $\langle \mathbf{x} \rangle$  with a 4-dimensional Gaussian probability distribution given by  $S$ . Four random numbers select the final phase space vector for the particle out of this distribution.

The phase space vector  $\mathbf{x}(s)$  propagates as

$$\mathbf{x}(s) = \mathbf{R}(s, s') \mathbf{x}(s') \quad (8)$$

in the absence of fluctuations. Elements of the matrix  $\mathbf{R}$  satisfy

$$\frac{d^2}{ds^2} R_{1j} + \gamma_x(s) \frac{d}{ds} R_{1j} + \omega_x^2(s) R_{1j} + \omega_c^2(s) R_{3j} = 0 , \quad (9a)$$

$$\frac{d^2}{ds^2} R_{3j} + \gamma_y(s) \frac{d}{ds} R_{3j} + \omega_y^2(s) R_{3j} + \omega_c^2(s) R_{1j} = 0 , \quad (9b)$$

$$R_{2j} = \frac{d}{ds} R_{1j}, \quad \text{and} \quad R_{4j} = \frac{d}{ds} R_{3j} \quad (9c)$$

with the initial condition  $\mathbf{R}(s = s', s') = \mathbf{I}$ . The index  $j = 1, \dots, 4$ ,  $\gamma_x$  and  $\gamma_y$  are the damping rates,  $\omega_x$  and  $\omega_y$  are the uncoupled betatron frequencies, and  $\omega_c$  is the coupling frequency.

The matrix  $\mathbf{R}$  is important for determining both  $\langle \mathbf{x} \rangle$  and  $\mathbf{S}$ . If the length of the arc between interaction points is  $L$ , then

$$\langle \mathbf{x} \rangle = \mathbf{R}(L, 0) \mathbf{x}_0 . \quad (10)$$

The phase space vector at  $s$  due to photons emitted at  $s'$  is

$$\mathbf{x}(s) = \mathbf{R}(s, s') \mathbf{F}(s') \quad (11)$$

where  $\mathbf{F}(s')$  is related to the dispersion ( $\eta_1 = \eta_x, \dots, \eta_4 = d\eta_y/ds$ ) and photon spectrum ( $n(u, s')$ ) at  $s'$

$$\mathbf{F}_j(s') = - \eta_j(s') \int_0^{\frac{u}{E_0}} n(u, s') du . \quad (12)$$

Modelling the radiation as white noise gives

$$\mathbf{S} \approx \int_0^L \mathbf{R}(L, s') \mathbf{F}(s') \mathbf{F}^T(s') \mathbf{R}^T(L, s') ds' . \quad (13)$$

A detailed lattice description including skew quadrupoles is needed to solve eqs. (9) for  $\mathbf{R}$ . A smooth approximation that follows from the work of Chandrasekhar[17] was used for the DCI simulations reported in this paper. The frequencies and damping were taken as independent of  $s$ , and the damping was set equal in the two dimensions. Equations (9a) and (9b) become

$$\frac{d^2}{ds^2} R_{1j} + \frac{2}{\tau} \frac{d}{ds} R_{1j} + \omega_x^2 R_{1j} + \omega_c^2 R_{3j} = 0 , \quad (14a)$$

and

$$\frac{d^2}{ds^2} R_{3j} + \frac{2}{\tau} \frac{d}{ds} R_{3j} + \omega_y^2 R_{3j} + \omega_c^2 R_{1j} = 0 . \quad (14b)$$

The matrix  $\mathbf{R}$  given by eqs. (14) and (9c) depends on the betatron frequencies, coupling frequency, and damping time. The matrix  $\mathbf{S}$  depends on the dispersion and radiation spectrum in addition. These are taken as independent of  $s'$  in this smooth approximation, and, having made this approximation, the numerical values of  $\mathbf{F}$  are determined by the nominal beam emittances through eq. (13) in the limit  $L \rightarrow \infty$ .

The input parameters are the emittances away from the coupling resonance and the coupling resonance width. The results of a simulation of synchrotron radiation without the beam-beam interaction are shown in Figure 1. When  $|Q_x - Q_y| > \Delta Q$ , the coupling resonance width, the beam sizes are those expected from the emittance ratio. When  $|Q_x - Q_y| \leq \Delta Q$  coupling decreases the horizontal size and increases the vertical size making them equal for  $Q_x = Q_y$ .

The principal advantage of this technique of simulating radiation is that x-y coupling is not included in an *ad hoc* manner. Instead it is part of the model of the arc, and it affects the motion and radiation of individual particles differently. This could be important in DCI where the emittances away from the coupling resonance are substantially different and the beam-beam tune spread is much larger than the coupling resonance width. However, as mentioned at the end of the next section, it was not.

#### IV. PERFORMANCE AT $\bar{q} = 0.725$

There are two beam DCI data near the coupling resonance for  $0.70 < \bar{q} < 0.82$ [6,7,18] where  $\bar{q}$  is defined as  $\bar{q} = [q_x + q_y]/2$ . Figure 2 shows that the measured beam-beam strength parameter at  $\bar{q} = 0.725$  saturates at  $\xi = 0.018$ . The strength parameter was determined from luminosity and beam current measurements using eq. (3). The systematic error is estimated to be  $\pm 10\%$ [10]. These data can be interpreted in terms of beam-beam resonances.

##### IV.1 Phase Advance Errors

The resonances for a round beam are  $2p\bar{q} = n$  where  $p$  and  $n$  are integers. The resonance strengths depend on the resonance order,  $2p$ , and the lattice symmetry through the parity of  $n$ .

The reduced Hamiltonian when there is a betatron phase error between IR's is derived in Appendix A. It is

$$H_{\text{red}} = H_0 + \varepsilon \omega_0 \left[ T_0(I) + \left\{ 1 + (-1)^n (1 + 4i\pi p \Delta Q) \right\} \times T_{2p}(I) \right] \quad (15)$$

where  $\varepsilon = Nr_e/\gamma$ , the functions  $T_k$  of the action,  $I$ , are given by eq. (A6), and  $2\pi\Delta Q$  is the phase advance error between IR's. The resonance term,  $\{ \} \times T_{2p}(I)$ , decreases as the resonance order increases, and  $n$  determines the dependence on  $\Delta Q$ . If  $n$  is even, the resonance term is large and approximately independent of  $\Delta Q$ , but if  $n$  is odd, the leading order terms multiplying  $T_{2p}$  cancel and the resonance term is proportional to  $\Delta Q$ . The operating point  $\bar{q} = 0.725$  is just below the  $4\bar{q} = 3$  and  $8\bar{q} = 6$  resonances. Without phase advance errors, the eighth order resonance would be the dominant one, but with phase advance errors the fourth order resonance could be important.

The DCI quadrupoles were not measured, but, from experience with SUPER-ACO, it is estimated that the rms gradient error was 0.1% [10]. A Monte Carlo calculation was performed to estimate the effect of such gradient errors. The DCI lattice was used, and the tunes for each trial were adjusted to the nominal values ( $Q_y = 1.725$ ,  $Q_x = 3.725$ ) by overall changes to the horizontal and vertical quadrupoles. The phase advance errors between IR's was then calculated. The results were  $\sigma(\Delta Q_x) = 7.2 \times 10^{-4}$ ,  $\sigma(\Delta Q_y) = 1.9 \times 10^{-3}$ , and the correlation coefficient was -0.74. The beam-beam simulation discussed below used  $\Delta Q_x = -0.001$  and  $\Delta Q_y = 0.004$ . This would be roughly a two standard deviation effect if the rms gradient error was 0.1%.

Figure 3 shows the results of simulations of TWO with and without phase advance errors. These results were obtained by starting at the lowest value of the current,  $I = 3$  mA, and tracking for about 1.05 betatron damping times ( $1.5 \times 10^5$  turns). The test particle locations were saved and used to begin a run at the next current. This was continued until the highest current of 21 mA was reached. The runs with phase advance errors and  $I = 19$  mA, 21 mA were tracked for 2.2 betatron damping times. The luminosity,  $\xi$ , and emittances reached stable values that varied by  $\pm 2\%$  or less every 12,500 turns at all currents. The horizontal and vertical sizes of each beam were equal,  $\sigma_{x1} = \sigma_{y1}$  and  $\sigma_{x2} = \sigma_{y2}$ . There were no indications of flip-flop phenomena; the relative sizes satisfied  $0.95 \leq \sigma_{x1}/\sigma_{x2} \leq 1.05$  at all currents. There was no transverse feedback

and the rms center-of-mass motion was about 20% of the beam size. The two beams moved in phase, and the test discussed below for ONE indicated that the feedback described in Section III.1 would not change the results.

The simulation results with  $\Delta Q = 0$  are well above the data, but with phase advance errors the dependence of  $\xi$  on current and the saturation value  $\xi = 0.020$  are consistent with the data within the 10% systematic error. We conclude that the DCI performance at  $\bar{q} = 0.725$  can be explained with reasonable phase advance errors. Piwinski has pointed out the importance of optical errors in PETRA[19], and this result for DCI reinforces his conclusion. Phase advance errors are not likely to be as important in single interaction region colliders where tunes can be measured well and adjusted to remove errors.

#### IV.2 Radiation Damping

Prior to studying the effects of phase advance errors and reaching the conclusion above, we performed some simulations of ONE with  $\bar{q} = 0.8625$  (giving the same phase advance between IR's as  $Q_x = 3.725$ ,  $Q_y = 1.725$  did in DCI) and different amounts of radiation damping. Phase advance errors are not possible because the model has only one IR, and the results address some of the effects of radiation damping on beam-beam performance. Figure 4 shows the dependence of the beam-beam strength parameter on current for different damping decrements,  $\delta$ , defined as the ratio of the energy loss between collisions to the beam energy. The radiation fluctuations were changed to give the same emittances for different damping decrements. The beam-beam performance at this operating point is only weakly dependent on  $\delta$ . Tune scans at a fixed current near the  $\bar{q} = 7/8$  resonance are shown in Figure 5. Far from the resonance the dependence on  $\delta$  is weak. Near the resonance the behavior is more complex, however. There is a substantial change between  $\delta = 2 \times 10^{-5}$  and  $\delta = 5 \times 10^{-5}$  but only small changes for  $\delta < 2 \times 10^{-5}$ .

These results are not consistent with diffusion models[20] that predict radiation effects that are insensitive to the tune. Keil and Talman[21], Seeman[22], and Rice[23] have looked at the effects of radiation damping in operating storage rings. A direct comparison with their work is not possible for two reasons. First, they use experimentally determined beam-beam limits that

can depend on the beam halo as well as the core. Our work studies only the core because it is restricted to a small number of test particles and a small number of damping times. Second, the data are at a variety of operating points, but our simulation results show that the operating point is a crucial parameter. We conclude that beam-beam performance is only weakly dependent on radiation damping away from low order resonances.

Two checks were performed at  $I = 58$  mA (equivalent to  $I = 14.8$  mA in TWO) and  $\delta = 5 \times 10^{-6}$ . In the standard conditions there was no feedback and the synchrotron radiation was generated with the coupled model discussed in Section III.2;  $\xi = 0.0220$  for those conditions. With feedback we found  $\xi = 0.0221$ , and with the horizontal and vertical emittances generated independently  $\xi = 0.0228$ . We conclude that the results are not sensitive to feedback or the modelling of synchrotron radiation.

#### V. PERFORMANCE AT $\bar{q} = 0.790 - 0.800$

The maximum  $\xi$  was measured as a function of tune in the region  $\bar{q} = 0.790 - 0.800$ ; the results are presented in Figure 6[7]. The eyeball fit to the data goes to  $\xi = 0$  at  $\bar{q} = 9/11$ . This is an interesting region to study with simulations. The lowest order resonance that satisfies the resonance condition  $2p\bar{q} = n$  is  $\bar{q} = 8/10$ , and the reduced Hamiltonian (eq. (15)) suggests that the resonance strength is independent of  $\Delta Q$ . It was anticipated that these data would be difficult to interpret with the resonance model in Appendix A because:

- 1) the tenth order resonance should not have any effect above  $\bar{q} = 0.800$  and yet there is one measurement at  $\bar{q} = 0.803$  that is consistent with the trend of the data. The tune and luminosity measurements at this point are correct[10].
- 2)  $\bar{q} = 9/11$  does not arise naturally because it is an odd order resonance. Odd order resonances can appear if the beams do not collide head-on, but if that were the case one would expect the  $\bar{q} = 4/5$  resonance to be stronger than  $\bar{q} = 9/11$ .

Simulations of TWO were performed at  $\bar{q} = 0.7900, 0.7933, 0.7950, 0.7967, \text{ and } 0.8000$ ; the results are in Figure 7. These runs were performed with  $\Delta Q_x = -0.001, \Delta Q_y = 0.004$ , and feedback. The latter was an arbitrary choice at the time because feedback did not affect



performance at  $\bar{q} = 0.725$ . The runs at low currents were 2.1 damping times long, and the behavior was similar to that at  $\bar{q} = 0.725$  and low currents. The luminosity,  $\xi$ , and the emittances were stable, and the beam sizes were approximately equal. The striking difference was at high currents and all tunes except  $\bar{q} = 0.800$ ; the beam sizes became unequal (a flip-flop state) and that lowered  $\mathcal{L}$  and  $\xi$  abruptly rather than saturating gently as at  $\bar{q} = 0.725$ . As one example, at  $\bar{q} = 0.795$  and  $I = 30$  mA the results were  $\mathcal{L} = 1.10 \times 10^{29} \text{cm}^{-2} \text{s}^{-1}$ ,  $\xi = 0.0184$ , and  $\sigma_{x1}/\sigma_{x2} = 1.04$ , but at 35 mA  $\mathcal{L} = 0.62 \times 10^{29} \text{cm}^{-2} \text{s}^{-1}$ ,  $\xi = 0.0089$ , and  $\sigma_{x1}/\sigma_{x2} = 2.08$  after 4.2 damping times. These values were not stable even after that length of time. The flip-flop state did not occur at  $\bar{q} = 0.800$ . The results for the maximum  $\xi$ 's based on Figure 7 are inconsistent with the data in Figure 6. We conclude that there must be additional important physics in this operating region.

Studies were performed to identify important factors. The effects of optical errors were checked by setting  $\Delta Q_x = \Delta Q_y = 0$  at  $\bar{q} = 0.7933$  and  $\bar{q} = 0.7967$ ; the feedback was left on. The results were unchanged. The low current behavior was the same and flip-flops occurred at the same values of current. The feedback was turned-off and current scans performed at  $\bar{q} = 0.7950$ ,  $0.7967$ , and  $0.8000$  with  $\Delta Q_x = -0.001$  and  $\Delta Q_y = 0.004$ . The results were strikingly different because the flip-flop states did not occur. This leads us to believe that coherent effects are important in this tune region. A more complete exploration would require using a field calculation algorithm that does not assume a Gaussian charge distribution. We have developed such an algorithm[4], but applying it to DCI with its long damping time would be prohibitive because of required computer resources.

## VI. SUMMARY AND CONCLUSIONS

DCI performance with two beams at  $\bar{q} = 0.725$  can be understood with a reasonable phase advance error between the interaction regions. The importance of such errors was first discussed by Piwinski for PETRA[19]. Studies show that the effects of radiation damping near this tune depend on the proximity of resonances. The behavior at  $\bar{q} = 0.795$  is more difficult to understand. It is outside the single particle Hamiltonian model presented in Appendix A and used to explain the results at  $\bar{q} = 0.725$ . There is additional important physics and some

indication that coherent effects are responsible. These are expected to be important at low values of damping as in DCI[4], and it is widely believed that coherent effects were the cause of the failure of the space charge compensation experiments in DCI[24].

What do these results imply about heavy quark factories? There optical errors will not be present because there will be only one interaction region and the radiation damping will be considerably stronger than at DCI making coherent effects less important. We still consider round beams to offer an exciting possibility for high luminosity and look forward to their use in the Novosibirsk  $\Phi$ -factory.

We enjoyed and appreciate the discussions about DCI with J. Le Duff, M. P. Level, P. C. Marin, E. M. Sommer, and H. Zyngier. This work was supported by the Department of Energy, contracts DE-AC03-76SF00098 and DE-AC03-76SF00515. Early work on this topic was performed at the Laboratory of Nuclear Studies, Cornell University, which is supported by the National Science Foundation.

#### APPENDIX A: ANALYSIS OF BETATRON PHASE ERRORS

This appendix follows closely the Hamiltonian analysis of bunch length effects in the beam-beam interaction[9]. Consider the motion of a particle that collides with a beam of  $N$  particles at two diametrically opposite interaction regions (IR's). The total Hamiltonian is

$$H(x, p_x, t) = H_0(x, p_x) + \varepsilon \sum_{n=-\infty}^{\infty} \int_0^1 \frac{d\eta}{\eta} \left[ 1 - \exp\left[-\frac{\eta}{2} \left(\frac{x}{\sigma_\beta}\right)^2\right] \right] \times \left[ \delta(t - nT_0) + \delta(t - nT_0 - T_0/2) \right] \quad (A1)$$

where  $x$  is the transverse coordinate and  $p_x$  is the conjugate momentum. The unperturbed betatron motion is described by  $H_0$ , and the perturbation parameter is  $\varepsilon = Nr_e/\gamma$ . The beam-beam potential is that produced by a round beam with rms transverse width  $\sigma_\beta$ . The sum is over all turns, and the two  $\delta$ -functions describe the two interaction points. Synchrotron motion and

bunch length effects are ignored in equation (A1), so this analysis holds for bunch lengths much shorter than  $\beta^*$ , the interaction region  $\beta$ -function.

Transform the Hamiltonian to the action-angle coordinates of  $H_0$ ,  $I$  and  $\psi$ , given by[25]

$$x = \sqrt{2I\beta(t)} \cos(\psi + \chi(t)), \quad (\text{A2})$$

and

$$\chi(t) = c \int_0^t \frac{dt}{\beta(t)} - \omega_0 Q_\beta t \quad (\text{A3})$$

where  $Q_\beta$  is the betatron tune for one complete revolution and  $\omega_0 = 2\pi/T_0$ . The angle  $\chi(t)$  is the deviation from a smooth betatron phase advance. If there is a betatron phase error between interaction regions, i.e. if the phase advance from the first to the second IR is  $2\pi(Q_\beta/2 + \Delta Q)$  and the phase advance from the second to the first IR is  $2\pi(Q_\beta/2 - \Delta Q)$ ,

$$\chi(nT_0) = 0, \text{ and } \chi(nT_0 + T_0/2) = 2\pi\Delta Q. \quad (\text{A4})$$

Fourier analyzing the Hamiltonian in time and  $\psi$  and making a change of variables gives[9]

$$H = H_0 + \quad (\text{A5})$$

$$\varepsilon\omega_0 \sum_{n,p=-\infty}^{\infty} T_{2p}(I) \left[ 1 + \exp(i\pi(n+4p\Delta Q)) \right] \exp(i(n\omega_0 t - 2p\psi))$$

where

$$T_k(I) = \frac{1}{(2\pi)^2} \int_0^{2\pi} \frac{d\theta}{\eta} \int_0^1 \left[ 1 - \exp[-\eta \cos^2 \theta] \right] e^{-ik\theta} d\eta. \quad (\text{A6})$$

The function  $T_k$  equals zero when  $k$  is odd, so there are only even  $k$  terms in eq. (A5). Near a single isolated resonance,  $2pQ_\beta = n$ , the reduced Hamiltonian is

$$\begin{aligned} H_{\text{red}} &= H_0 + \varepsilon\omega_0 \left[ T_0(I) + T_{2p}(I) \left\{ 1 + \exp(i\pi(n+4p\Delta Q)) \right\} \right] \\ &= H_0 + \varepsilon\omega_0 \left[ T_0(I) + \left\{ 1 + (-1)^n (1 + 4i\pi p\Delta Q) \right\} \times T_{2p}(I) \right]. \end{aligned} \quad (\text{A7})$$

A slowly varying phase factor that multiplies  $T_{2p}$  has been neglected in eq. (A7). The partial derivative  $\partial T_0 / \partial I$  gives the tune shift with action, and  $\{ \} \times T_{2p}(I)$  is the resonance term.

The dependence on  $\Delta Q$  is determined by  $n$ . If  $n$  is even, the resonance term is large and approximately independent of  $\Delta Q$

$$H_{\text{red}} = H_0 + \epsilon \omega_0 \left[ T_0(I) + 2T_{2p}(I) \right], \quad (\text{A8})$$

and the phase advance error does not affect resonance strength. However, when  $n$  is odd the leading order terms multiplying  $T_{2p}$  cancel and the resonance term is proportional to  $\Delta Q$ . The reduced Hamiltonian is

$$H_{\text{red}} = H_0 + \epsilon \omega_0 \left[ T_0(I) - 4i\pi p \Delta Q T_{2p}(I) \right], \quad (\text{A9})$$

and the resonance widths in action and frequency[26] are proportional to  $(\Delta Q)^{1/2}$ .

TABLE I: PARAMETERS

		DCI[7]	ONE	TWO
Revolution frequency (MHz)		3.169	6.338	3.169
Bending radii (m)	horizontal	3.8197	--	--
	vertical	-4.0627, 4.0852	--	--
Superperiods		2	1	2
Bunches/beam		1	1	1
Interaction regions		2	1	2
RF frequency (MHz)		25.352	--	--
Harmonic number		8	--	--
Momentum compaction		0.0788	--	--
Tunes	horizontal	3.725*	1.8625*	3.725*
	vertical	1.725*	1.8625*	3.725*
$\beta^*$ (m)	horizontal	2.18	2.18	2.18
	vertical	2.18	2.18	2.18
$\eta^*$ (m)	horizontal	-0.21	0.00	0.00
	vertical	0.69	0.00	0.00
Coupling Resonance width		0.001 - 0.003[10]	0.001	0.002
Energy (MeV)		1000.	800.	1000.
Energy loss per turn (keV)		28.	11.5	20.*
Damping decrement ( $\times 10^{-6}$ )		14.	7.1	10.*
Damping times (msec)	horiz.	31.	61.	32.*
	vert.	22.	43.	32.*
	long.	10.	20.	--
RMS energy width ( $\times 10^{-4}$ )		4.1	3.3	--
RF voltage (kV)		250.[27]	--	--
Bunch length (m)		0.097	--	--
Beam sizes (mm)				
	No coupling			
	horiz.	0.984	0.787	0.976
	vert.	0.360	0.291	0.225
	With coupling			
	horiz.	0.714	0.573	0.708
	vert.	0.763	0.613	0.708
Natural emittances ( $\mu\text{m}$ )	horiz.	0.441	0.282	0.437
	vert.	0.0235	0.0150	0.0233

\* => Variable - the given values are nominal ones.

-- => Values unknown or not used in simulations.

## REFERENCES AND FOOTNOTES

1. S. Krishnagopal and R. Siemann, *Proc 1989 IEEE Part Accel Conf*, 836 (1989).
2. S. Peggs and R. Talman, *Phys Rev D* **24**, 2379 (1981).
3. M. Bergher et al, *IEEE Trans Nucl Sci NS-26*, 3559 (1979).
4. S. Krishnagopal and R. Siemann, "Coherent Beam-Beam Interactions in Electron-Positron Colliders", SLAC-PUB-5630, LBL-31145 (SLAC, LBL, 1991).
5. It is assumed that  $R_\sigma \leq 1$ . If  $\sigma_y > \sigma_x$  as it is in DCI, the appropriate definition is  $R_\sigma = \sigma_x/\sigma_y$ .
6. R. Chehab et al, *Proc of 11th Inter Conf on High-Energy Accel*, 702 (1980).
7. J. Le Duff and M. P. Level, "Experiences Faisceau-Faisceau sur DCI", LAL/RT/80-03 (Orsay, 1980).
8. F. M. Izrailev and I. B. Vasserman, *Proc 7th All Union Conf on Charged Part Accel*, 288 (1980).
9. S. Krishnagopal and R. Siemann, *Phys Rev D* **41**, 2312 (1990).
10. J. Le Duff, M. P. Level, P. Marin, E. M. Sommer, and H. Zyngier, private communication.
11. M. Bassetti and G. Erskine, CERN-ISR-TH/80-06 (CERN, 1980).
12. Y. Okamoto and R. Talman, CBN 80-13 (Cornell, 1980).
13. R. E. Greenwood and J. J. Miller, *Amer Math Soc Bull* **54**, 765 (1948).
14. M. Abramowitz and I. A. Stegun, *Handbook of Mathematical Functions*, National Bureau of Standards, eq. 7.1.3.
15. J. F. Schonfeld, *Ann Phys* **160**, 241 (1985).
16. S. Krishnagopal and R. Siemann, CBN 88-8 (Cornell, 1988).  
R. Siemann, CBN 89-2 (Cornell, 1989).
17. S. Chandrasekhar, *Rev Mod Phys* **15**, 1 (1943).
18. These tunes are far from the optimum operating points in ref. 1 which for two interaction regions would be just above the integer and just above the half-integer.
19. A. Piwinski, *IEEE Trans Nucl Sci NS-30*, 2378 (1983).
20. see A. Chao, *AIP Conf Proc* **127**, 201 (1985) for a summary.

21. E. Keil and R. Talman, *Part Accel* **14**, 109 (1983).
22. J. Seeman, *Nonlinear Dynamics Aspects of Particle Accelerators* (Berlin: Springer-Verlag, 1986, edited by J. M. Jowett, S. Turner and M. Month), p. 121.
23. D. Rice, *Third Advanced ICFA Beam Dynamics Workshop* (Novosibirsk: INP, 1989, edited by I. Koop and G. Tumaikin), p. 17.
24. J. Le Duff et al, *Proc of 11th Inter Conf on High-Energy Accel*, 707 (1980).
25. R. Ruth, *AIP Conf Proc* **153**, 150(1987).
26. B. V. Chirikov, *Phys Rep* **52**, 263 (1979).
27. M. P. Level, "Collective Effects in DCI", LAL-RT-79/5 (Orsay, 1979).

#### FIGURE CAPTIONS

Figure 1: Simulation of synchrotron radiation in a storage ring approximating DCI with no beam-beam interaction. Storage ring parameters are:  $\beta_x = \beta_y = 2.18$  m,  $\epsilon_x = 0.23$   $\mu$ m,  $\epsilon_y = 0.023$   $\mu$ m,  $\sigma_x = 7.08 \times 10^{-4}$  m,  $\sigma_y = 2.24 \times 10^{-4}$  m,  $(Q_x + Q_y)/2 = 1.860$ , and  $\Delta Q$  (coupling resonance width) = 0.001.

Figure 2: The measured dependence of the beam-beam strength parameter on current. The currents of the two beams were equal,  $I_+ = I_- = I$ , and the line is an eyeball fit to the data.

Figure 3: Simulation results for TWO with and without phase advance errors. The values of  $\Delta Q_x$  and  $\Delta Q_y$  are discussed in the text. The curve is the line through the data in Figure 2.

Figure 4: Simulation results for ONE with different damping decrements. This operating point corresponds to  $\bar{q} = 0.725$  in TWO. The curve is the line through the data in Figure 2 scaled by  $1/0.256$  (Section II).

Figure 5: Tune scans for ONE with different damping decrements.

**Figure 6: Data from DCI - the maximum beam-beam strength parameter as a function of tune[7].**

**Figure 7: Simulation results for the dependence of  $\xi$  on current at different tunes when feedback was applied.**



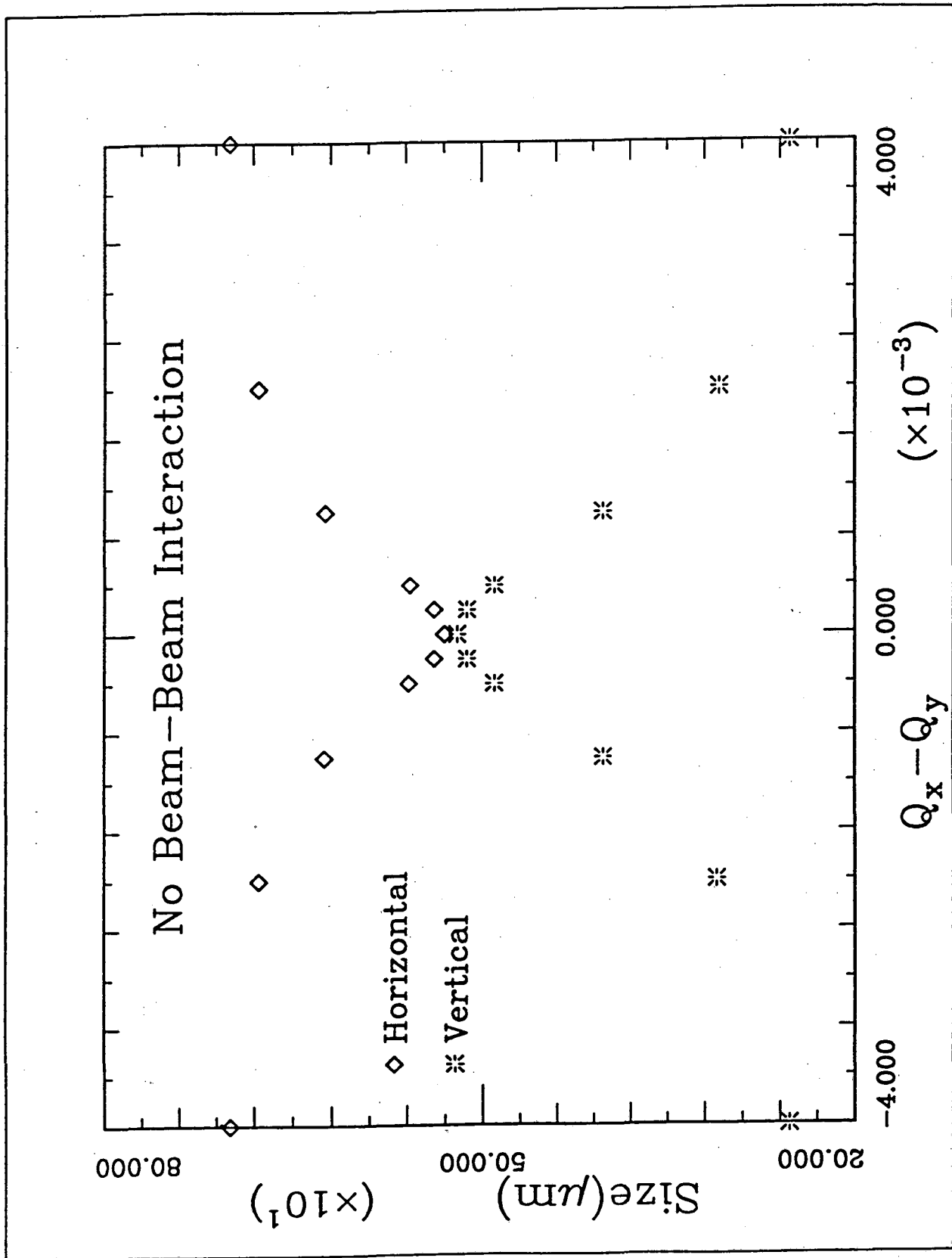


Figure 1

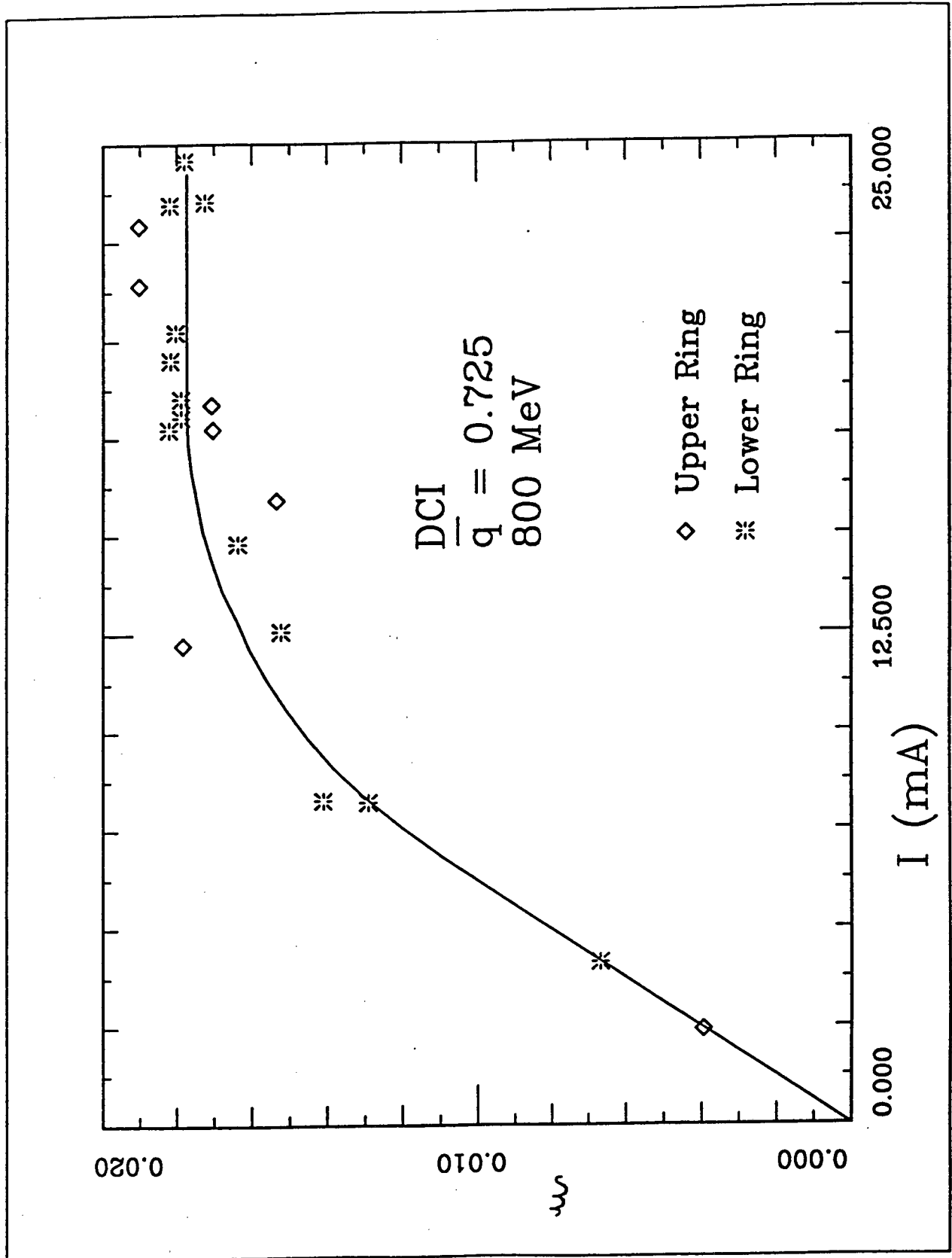


Figure 2

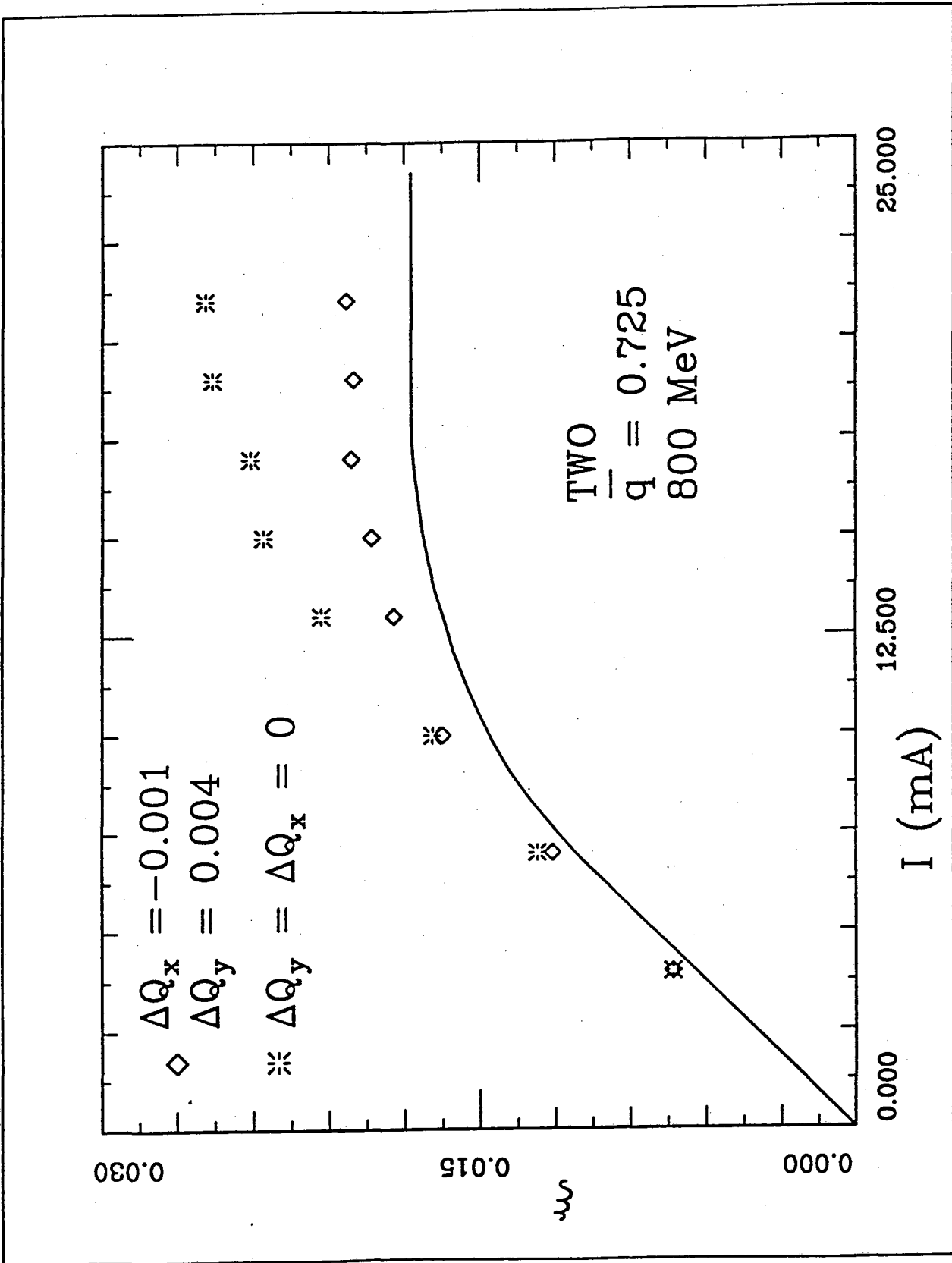


Figure 3

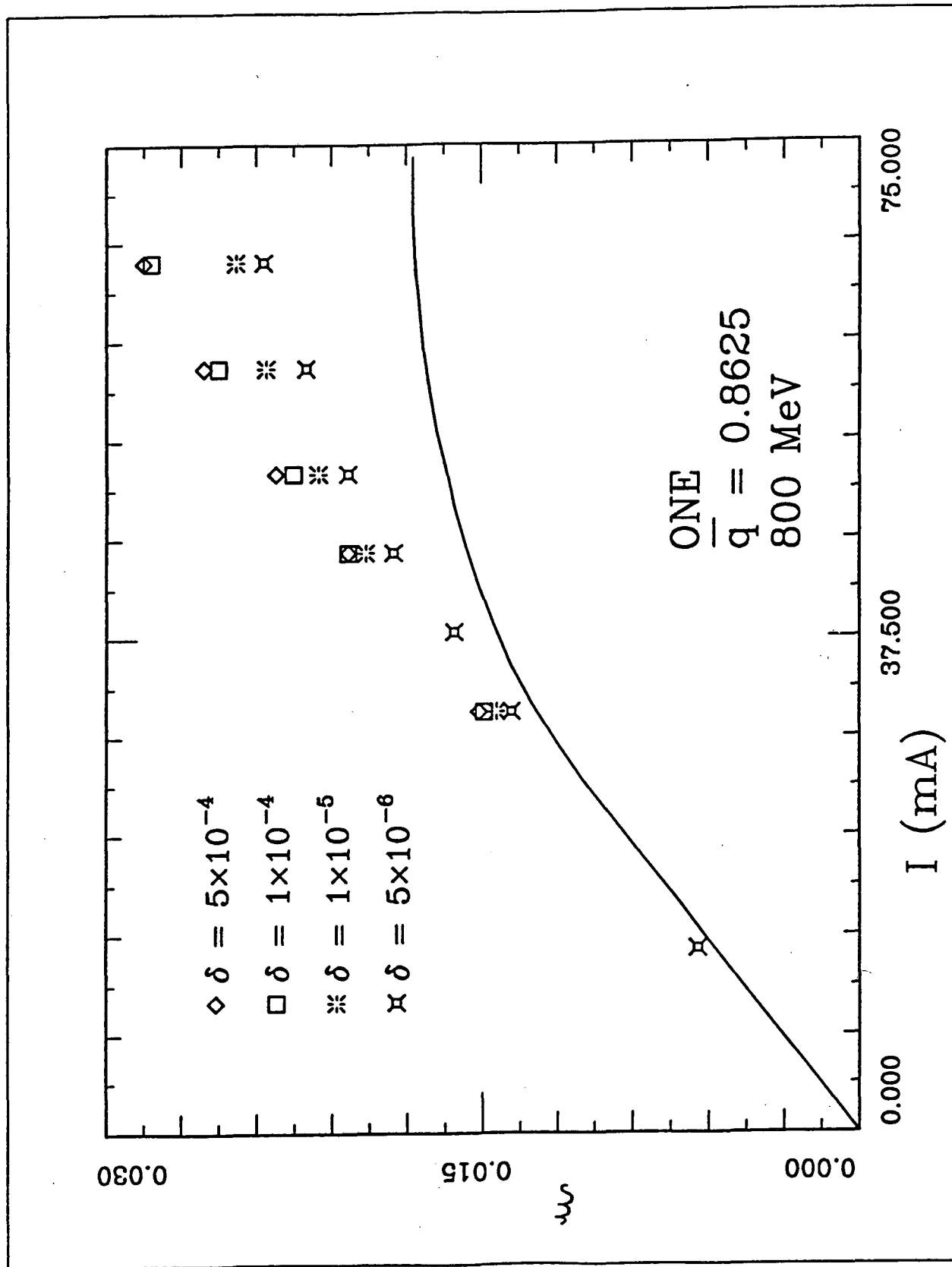


Figure 4

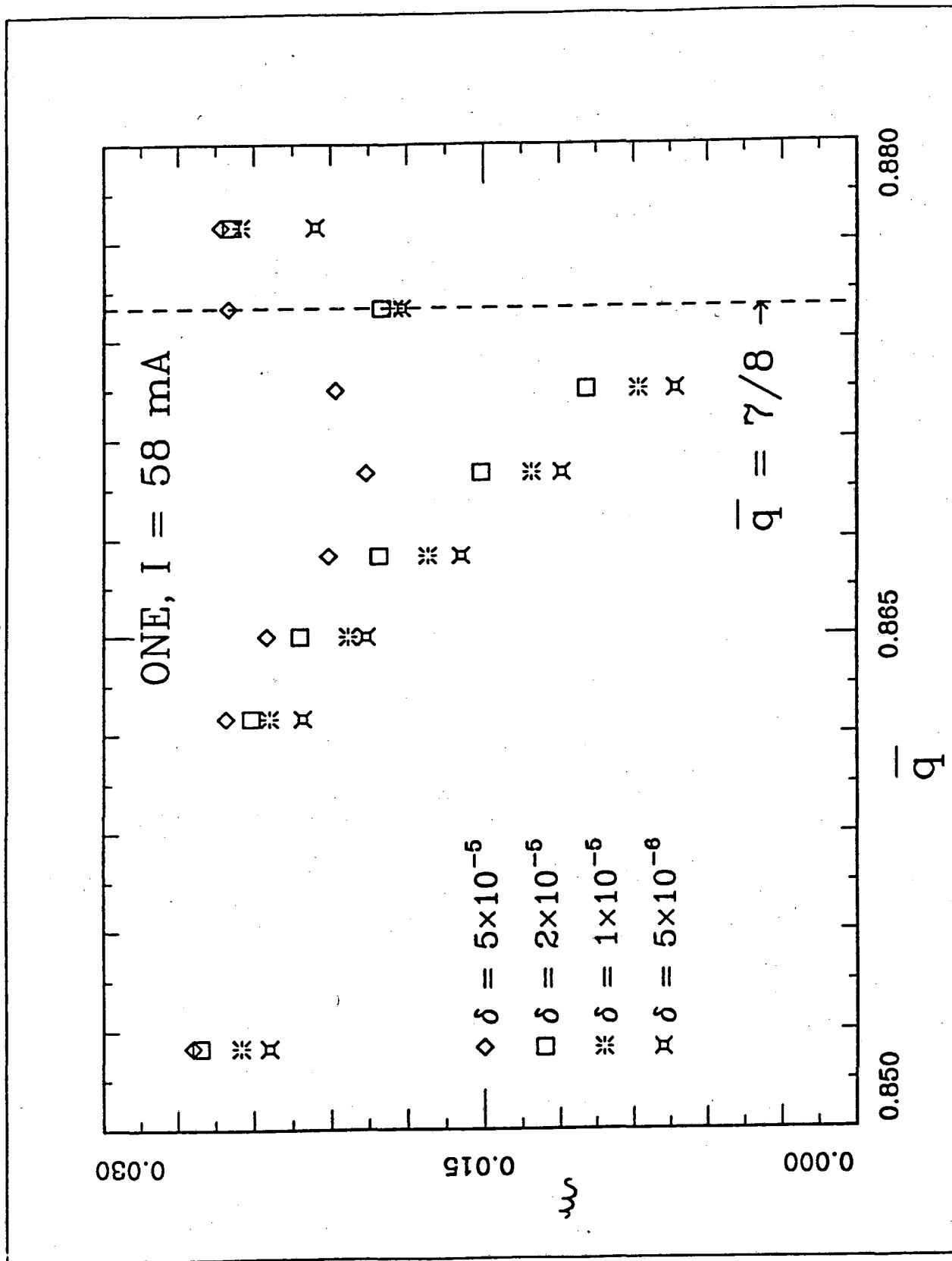


Figure 5

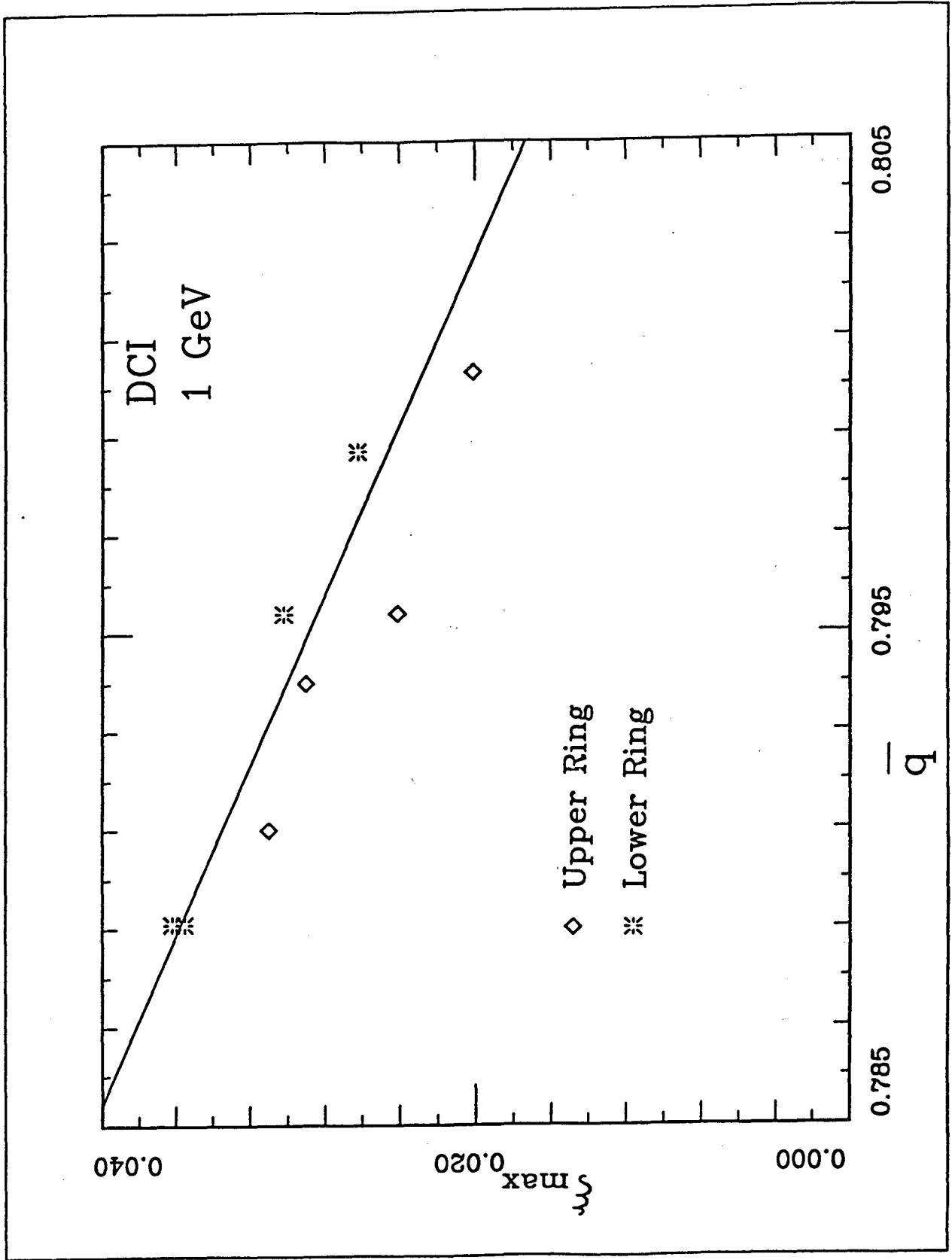


Figure 6

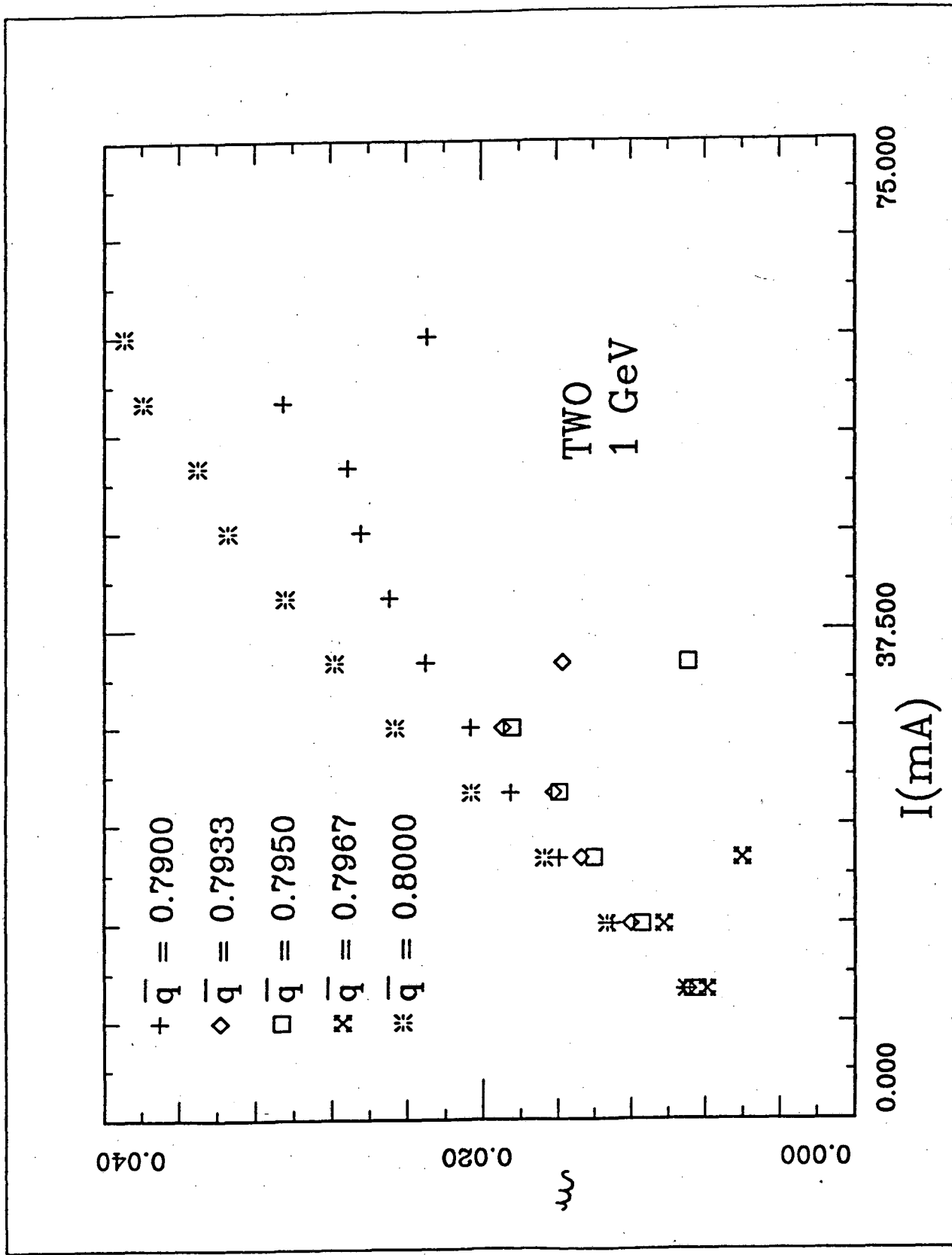


Figure 7

LAWRENCE BERKELEY LABORATORY  
UNIVERSITY OF CALIFORNIA  
INFORMATION RESOURCES DEPARTMENT  
BERKELEY, CALIFORNIA 94720